Ms. Ref. No.: TIV-D-17-00480

Characterization and reproducibility of HepG2 hanging drop spheroids Toxicology in Vitro

Tracey Hurrell[a, l] (PhD, tracey.hurrell@ki.se)

Andrea Antonio Ellero[a] (BSc Honors, andyellero@gmail.com)

Zelie Flavienne Masso[a] (BSc Honors, flaviennemasso@gmail.com)

Allan Duncan Cromarty[a] (PhD, duncan.cromarty@up.ac.za)

[a] Department of Pharmacology, Faculty of Health Sciences, School of Medicine, University of Pretoria, Private Bag X323, Arcadia, 0007, South Africa

[l] Section of Pharmacogenetics, Department of Physiology and Pharmacology, Karolinska Institutet, Nanna Svartz väg 2, 171 77 Stockholm, Sweden

Correspondence

Tracey Hurrell

Section of Pharmacogenetics
Department of Physiology and Pharmacology
Karolinska Institutet
Nanna Svartz väg 2
171 77 Stockholm, Sweden
tracey.hurrell@ki.se
+46-(0)8-524 877 62

Financial support

National Research Foundation Thuthuka Funding Scheme (Grant No. 87880)

Abstract

Hepatotoxicity remains a major challenge in drug development despite preclinical toxicity screening using hepatocytes of human origin. To overcome some limitations of reproducing the hepatic phenotype, more structurally and functionally authentic cultures *in vitro* can be introduced by growing cells in 3D spheroid cultures. Characterisation and reproducibility of HepG2 spheroid cultures using a high-throughput hanging drop technique was performed and features contributing to potential phenotypic variation highlighted. Cultured HepG2 cells were seeded into Perfecta 3D® 96-well hanging drop plates and assessed over time for morphology, viability, cell cycle distribution, protein content and protein-mass profiles. Divergent aspects which were assessed included cell stocks, seeding density, volume of culture medium and use of extracellular matrix additives. Hanging drops are advantageous due to no complex culture matrix being present, enabling background free extractions for downstream experimentation. Varying characteristics were observed across cell stocks and batches, seeding density, culture medium volume and extracellular matrix when using immortalised HepG2 cells. These factors contribute to wide-ranging cellular responses and highlights concerns with respect to generating reproducible characteristics in hanging drop spheroids.

Highlights

- Immortalized cell lines do not produce homogenous spheroid characteristics
- Protein content of HepG2 spheroids in hanging drops is influenced by medium volume
- Spheroid morphology is altered with the addition of artificial ECM
- Spheroid cultures alter the cell proliferation index and protein-mass profile

Keywords

HepG2 cells; hepatotoxicity; spheroids; hanging drops.

Introduction

More than 900 drugs, herbs and toxins have been reported to result in drug induced liver injury (DILI) with approximately 30-50% of reported acute hepatic failure being as a result of commercially approved drugs (Kola and Landis 2004, Nilesh, Ozick et al. 2011). Despite preclinical toxicity screening using hepatocytes of human origin, hepatotoxicity remains a major challenge in drug development. Tissue structure and geometry influence the '*bio-mimetic microenvironment*' and ultimately dictate cellular functionality (Bhadriraju and Chen 2002, Peters 2005). Adherent cell monolayers have played a fundamental role in understanding developmental biology, tissue morphogenesis, disease mechanisms, drug discovery and safety pharmacology. However, features of monolayer cultures such as unlimited nutrient access, altered cellular morphology and polarity, lack of cell-cell and cell-matrix interactions augment classic cellular responses. The artificial microenvironment offers poor physiological comparison, reducing the predictive power and correlation to *in vivo* responses (Bhadriraju and Chen 2002, Pampaloni, Reynaud et al. 2007).

To overcome of these limitations, cells can be grown in three-dimensional (3D) spheroids producing more structurally and functionally authentic cultures. Mimicking these higher order processes requires using single cells (~10 µm) to create functional hierarchical structures (100 µm - 1 mm)(Khetani and Bhatia 2008). Advances in tissue engineering have greatly improved the diversity of spheroid culture techniques. Static and dynamic culture approaches to produce spheroids include gel sandwich cultures, ultra-low attachment surfaces, hanging drop plates, solid scaffolds, hydrogel encapsulation, rotary cultures, microfluidic devices and bioreactors (Bhadriraju and Chen 2002, Kim 2005, Fey and Wrzesinski 2012, Shin, Park et al. 2012). Depending on the method of culture, spheroids have been shown to mimic the performance of tissues with protein levels which can rival those seen *in vivo* (Wrzesinski, Rogowska-Wrzesinska et al. 2014).

The complexity, cost and accuracy of hepatotoxic prediction dictate the applicability of each spheroid model while high-throughput is essential in drug discovery (Costa, Sarmento et al. 2014). Hanging drop spheroidal cultures are a static, extracellular matrix-free culture technique which allow cells to aggregate due to gravity. This model is relatively straightforward to culture and easily manipulated for experimental purposes (Teng 2015). With the aforementioned ease of manipulation, the extent to which the phenotype and growth characteristics of a specific cell type are altered is rarely adequately defined.

HepG2 cells spheroids (250 – 8000 cells), in the hanging drop system, have demonstrated potential in long term toxicity screening of compounds (Meuller et al. 2011). However, characterisation of larger spheroids, for experiments requiring more cell and protein mass, is limited. Well-defined preclinical toxicity screening systems are of vital importance to the pharmaceutical industry which require the ability to reliably reproduce the target phenotype (Bhadriraju and Chen 2002). This study reports on the reproducibility of HepG2 spheroids using a high-throughput strategy of hanging drop cultures including some features contributing to variation in growth characteristics and overall phenotype.

Materials and methods

HepG2 cell spheroid cultures

HepG2 human hepatoma cells were obtained from the American Tissue Culture Collection (ATCC #HB-8065; Manassas, USA), the European Collection of Authenticated Cell Cultures (ECACC; Wiltshire, UK: 85011430-1VL) and Cellonex (Johannesburg, RSA: CHG2-C). Cells were cultured in Eagle's Minimum Essential Medium (EMEM) supplemented with 10% foetal bovine serum (Gibco Lifeline Cell Technology, South America origin: FBS), 1% penicillin-streptomycin (10 000 U/ml penicillin and 10 000 µg/ml streptomycin) and 2 mM L-glutamine. Perfecta3D® 96-well hanging drop plates were used to generate spheroids. HepG2 cells were seeded between 10 000 to 50 000 cells per well in variable volumes (40 - 50 µl) of cell culture medium. Plates were incubated at 37°C with 5% CO_2 and assessed for up to 14 days. Partial medium exchange was done every alternate day and spheroids were harvested via air displacement.

Microscopy

Phase contrast images (EVOS FL Cell Imaging System or Zeiss AX10 microscope) were used to observe spheroid compaction and diameter over time. Live-dead staining of spheroids was done using fluorescein diacetate (FDA) and propidium iodide. Spheroids (n = 8), were collected by air displacement, centrifuged (200 *g*; 5 minutes) and washed with Hank's Balanced Salt Solution (HBSS). One millilitre of staining solution (10 µl of 2 mg/ml propidium iodide in HBSS and 2 µl of 5 mg/ml FDA in acetone) was used to stain spheroids for 5 minutes at room temperature. Spheroids were washed with HBSS and visualized using a Zeiss AX10 fluorescence microscope at an excitation wavelength of 488 nm and emission wavelengths of 535 nm and 620 nm. Digital images were recorded and then processed using ImageJ software.

Cell cycle analysis

Spheroids cultured for 10 days were collected (n = 20) and dissociated using 1 ml Accutase solution (Sigma-Aldrich; St Louis, USA) at 37°C for 45 minutes. Samples were resuspended in 200 µl PBS with 1% FBS and fixed in 3 ml of 70% ethanol. Samples were centrifuged (200 *g*; 5 minutes) and the pellet resuspended in 1 ml PI staining solution (40 µg/ml PI, 0.1% Triton X-10 and 100 µg/ml DNase free RNase) followed by incubation at 37°C for 40 minutes. Samples were analysed (n = 4 biological replicates) using a Cytomics FC500 (Beckman Coulter; Brea, USA) at an excitation of 488 nm and emission wavelength of 620 nm and fluorescence intensity monitored as histograms.

Protein collection

Spheroids (n = 10) were harvested, washed with PBS and lysed using 100 µl radioimmunoprecipitation buffer (10 mM Tris-HCL (pH 8), 1 mM ethylene diaminetetraacetic acid, 0.5 mM ethylene glycol tetraacetic acid, 1 % Triton X-100, 0.1% sodium dodecyl sulphate, 0.1% sodium deoxycholate, 140 mM sodium chloride) containing cOmplete™ protease inhibitor cocktail (Roche Pharmaceuticals; Basel, Switzerland). Cellular disruption was aided by ultrasonic disruption at 4°C (5 minutes with 30 second pulses at 1500 W), left on ice for 15 minutes, centrifuged at 4°C (16 000 *g*; 10 minutes). The supernatant protein concentration was quantified, in duplicate of a minimum of three biological replicates, using the bicinchoninic acid (BCA) assay using a 1:50 ratio of reagent B (4% copper II sulfate pentahydrate) to reagent A (2% sodium carbonate; 0.16% sodium tartrate; 0.9% sodium bicarbonate and 1% BCA; pH 11.25) with a 1:40 ratio of sample to reagent. Sample were incubated at 60°C in the dark for 30 minutes and quantified using an ELx800 Bio-Tek microplate reader at a wavelength of 560 nm.

SDS-PAGE based proteomics

Ten to twenty micrograms of protein in solution was mixed in a 1:1 ratio with Laemmli sample buffer (0.125 M Tris-HCL (pH 6.8), 4% SDS, 20% glycerol, 10% β-mercaptoethanol, and 0.004% bromophenol blue). Samples were heated to 95°C for 5 minutes, clarified by centrifugation at 16 000 *g* and loaded onto a Mini-PROTEAN TGX precast gradient polyacrylamide gel (4-15%; 10-wells: BioRad; California, USA). Gels were run (running buffer: 0.1% SDS, 25 mM Tris-base and 192 mM glycine) using a Mini-PROTEAN Tetra System (BioRad; California, USA) at 80 V for 15 minutes and 160 V until completion. Gels were stained using Coomassie brilliant blue (0.1% Coomassie brilliant blue R250, 50% methanol, 10% acetic acid in ddH_20) and visualized using a BioRad Gel Doc EZ Imager (BioRad; California, USA).

Statistics

Internal triplicates of three independent experiments per culture condition were conducted. Protein quantitation data was analysed using GraphPad Prism 5.0 and fold-changes calculated. Cell cycle histograms were initially analysed using deconvolution software (Wincycle Software; Washington, USA) following further analysis using GraphPad Prism 5.0 and the proliferation index calculated where

$$\text{Proliferation index} = (\text{S} + \text{G2/M}) \,/\, (\text{G0/G1} + \text{S} + \text{G2/M})$$

Results

The term spheroid is inconsistently used throughout literature and sometimes refers to loosely packed cellular aggregates which lack consistent cell-cell and cell-matrix interactions (Hirschhaeuser, Menne et al. 2010). Characterisation of spheroid morphology of breast and prostate cell lines suggest four distinct morphologies namely; round, mass, grape-like and stellate (Kenny, Lee et al. 2007, Härmä, Virtanen et al. 2010). These morphological characteristic cannot be directly compared to hanging drops where gravitational forces encourage cell aggregation.

HepG2 cells form three different origins (cell stocks 1 to 3) were used to culture spheroids, as hanging drops (Supplementary Figure 1), during this study. Despite a similar passage number, distinct differences in spheroid morphology were evident (Figure 1) for each cell stock. While the spheroids generated from all three cell stocks could be individually transferred without major disruption of their architecture, inconsistencies in compaction and diameter suggest varied degrees of cell-cell interactions.

The advantage of using hanging drops is that gravitational sedimentation is considered sufficient to drive aggregation with some extracellular matrices known to augment morphology. However, as tumour cells aberrantly express adhesion molecules, it is possible that aggregation and compaction may differ with the origin of the cell line and phenotype changes associated with passage number. This has implications for the phenotype of immortalized cells as well as responses to experimental perturbations. Based on access and number of early passage vials, cell stock 3 was used to assess the cell seeding density which was varied to investigate the effects of initial cell number on aggregation and compaction of a single spheroid over 10 days (Figure 2 and Supplementary Figure 2).

Spheroid compaction was observed from the decrease in spheroid diameter accompanied by an increase in cell density. However, the morphology of this cell stock appears categories HepG2 spheroids as tight aggregates more than compact spheroids. In addition, fluorescence microscopy illustrated homogenous FDA staining throughout spheroids with minimal PI staining suggesting that the spheroid maintained viable cells throughout the spheroid.

Time-course protein content

Protein content comparisons were performed using the three different HepG2 cell stocks using varying cell seeding densities and different culture times. HepG2 cells from stock 1 and stock 3 demonstrated a difference in overall protein content and variable increases of 2.94-fold and 4.65-fold, relative to protein content at day zero, when seeded at 10 000 cells per well in the same volume of medium (Figure 3). These spheroids, cultured in the same laboratory were purchased, at the lowest available passage, from two different sources. These variances highlight some limitations in comparing immortalised cell lines.

Liver phenotype modulation of HepG2 cells is influenced by cell culture density where low density cultures ($2x10^5$ cells/cm^2) exhibit a rapid doubling time and high density cultures ($1x10^6$ cells/cm^2) have a prolonged doubling time. This means that HepG2 cells can exhibit characteristics of foetal through to adult transitions depending on the duration of culture (Kelly and Darlington 1989). The variable fold-change between cell stocks of different origin suggests differences in growth characteristics, which may have been introduced during the initial cell amplification stage to provide sufficient cells for spheroid cultures where monolayer cultures of variable confluence were cultured. However, this limits the ability to compare maturation and experimental responses across cell stocks or batches which are supposed to represent a similar phenotype. When assessing variable seeding densities, an assumption may be that the protein content would increase in accordance with the increase in seeding density. This was not evident as protein content was 9.46 and 11.84 micrograms per spheroid for HepG2 cells seeded at 10 000 and 20 000 cells per well and cultured as spheroids for 7 days (Figure 3). This was accompanied by the observation that a higher seeding densities as well as culturing beyond 7 days was associated with a reduced fold-change in protein content.

Classically spheroids have three distinct zones which include an outer proliferation zone, intermediate quiescent zone of viable cells and a potential inner core where cells begin undergoing necrosis (Mehta, Hsiao et al. 2012).

Protein content over time could provide insight into the formation of spheroid zones. A reduced proliferative zone could be obtained at higher seeding densities reducing the increase in protein content due to a more rapid conversion to quiescence. The morphology observed in the spheroids assayed in this study did not demonstrate the classical spheroid architecture described. But from the data presented it is suggested that higher seeding densities the greater the extent of influence on the doubling time. As end-point protein concentration per spheroid could not provide insight into the growth kinetics, protein content was monitored at more regular intervals. A greater fold-change increase in protein content was observed for lower seeding densities over 10 days (Figure 4A).

Droplet volume also influenced end-point protein content (Figure 4B). Cultures seeded at lower volumes (40 µl) produced spheroids of lower protein content with a smaller fold-change in protein content observed. It is well established that some cultures grown in larger medium volumes proliferate faster with a greater cell yield (Ryan, Sharf et al. 1975). Therefore the resultant protein yield may be due to an inadequate availability of essential nutrients and growth factors from the medium due to the higher cellular burden. While HepG2 cells cultured in hanging drops are seeded in small medium volumes the proportional change in medium volume from 40 µl to 45 µl appears to be a noteworthy contributor to spheroid growth patterns. Based on the observations on protein content, spheroids were then consistently seeded at 45 µl at variable seeding densities for additional characterisation.

Cell cycle analysis

Cell growth can be characterized by exponential growth with a short doubling time, as seen in monolayer cell cultures or alternatively cells in tissue-like conglomerates or spheroids appear to reach a dynamic equilibrium with longer doubling times. These physiological attributes appear to be gained spontaneously (Wrzesinski, Rogowska-Wrzesinska et al. 2014) with potential zones of the spheroids showing various degrees of actively proliferating and quiescent but viable cells. This would have implications reproducibility and for preclinical models (Mehta G et al., 2012, Miyamoto Y et al., 2015). The number of cells transiting from the proliferation to quiescence or cell death could be influenced by initial seeding density. Speculatively, the lower the proliferation index, the more reminiscent cells would be of *in vivo* counterparts which are limited in their replicative potential.

Cell cycle analysis of disaggregated HepG2 spheroids showed a similar distribution of cell cycle to that of unsynchronized monolayer cultures with an increase in the G1 phase and minimal sub-G1 phase (Figure 5 and Table 1). This could be due to core cells transitioning to the stationary phase. The rate at which the G1 phase increase occurred was not assessed but, a similar pattern of increased G1 phase proportion was observed irrespective of the initial seeding density.

The variance in G1- and S-phase distribution and consequent impact on proliferation index could be due to spheroid geometry whereby weak cell-cell interactions occurred. Varied spatial geometry with seeding density alters the pathophysiological zonal gradients of classically characterised spheroids (Hirschhaeuser, Menne et al. 2010) and would consequently affect the proliferation index. Calculating the proliferation index (PI = (S+G2/M) / (G0/G1+S+G2/M)) showed that while the proliferation index was decreased in spheroids, the lower the seeding density the greater the reduction in proliferation index at 7 days while a higher proliferation index was observed at a higher seeding densities, after 7 days in culture. As indicated by the change in protein content, the timing associated with the most notably increase in protein content also varied. Seeding 10 000 cells per well showed the greatest increase in protein between day 7 and 10 whereas for 20 000 cells per well this was between day 3 and 7. This suggests that while all spheroids have a reduced proliferation index this index might fluctuate over the time as exponential cell growth phases differ across seeding densities.

SDS-PAGE based proteomics

In this study, differences in protein-mass profiles could be discerned between HepG2 monolayers and spheroids in some instances (Figure 6). However, these differences were transient and did not appear consistently across spheroid samples. This suggests that the transitions which alter equilibrium and maturation phases of the HepG2 phenotype within a certain cell stock are also highly batch dependent and altered across passage. Gel-based proteomics was not sensitive enough to distinguish differences in protein-mass profiles across different seeding densities but evidence for altering the proteome in spheroids is present.

HepG2/C3A cells cultured as monolayers and as spheroids have been assessed by other researchers at the times that cells transition from exponential to equilibrium phases. Altered proteins in spheroids include those governing cellular architecture and cytoskeletal rearrangement, metabolism, synthesis, oxygen levels, cell growth, transport, ubiquitination and protein degradation (Wrzesinski, Rogowska-Wrzesinska et al. 2014). Complex cellular and non-

cellular interactions govern the diverse liver functionality and augmentation of the proteome of HepG2 cells was evident but was not consistently achieved.

Extracellular matrices

Spheroid shape can be dictated by differential expression of E-cadherin and integrin's, which is influenced by cell type and ECM (Selden, Khalil et al. 1999, Lin, Chou et al. 2006). The transition from spontaneous cell aggregate requiring E- and N-cadherin to compact spheroids relying on surface integrin ß1-ECM interaction can be artificially reintroduced by collagen gels, laminin extracts and more complex matrices such as Matrigel (Selden, Khalil et al. 1999, Ivascu and Kubbies 2006).

Spheroid morphology and protein content were used to assess the influence of added artificial ECM in the form of methylcellulose and Matrigel. Cells were seeded (10 000 to 20 000 cells/well) in medium containing 0.5%, 1% and 2% methylcellulose or 0.5, 1.0, 2.0 and 4.0 mg/ml Matrigel. Diverse spheroid morphologies were observed while (Figure 7A-D) protein content of the resulting spheroids was similar in methylcellulose-based medium compared to ECM free cultures (Figure 7E). Increased viscosity negated gravitational forces which would normally allow cells to sediment to the droplet apex. Consequently, at higher concentrations of methylcellulose, multiple smaller spheroids formed as opposed to a single, concentric spheroid, increasing the heterogeneity of the technique. While aiding to droplet robustness, and having minimal influence on protein content, the use of methylcellulose promoted some compaction as seen by more defined spheroid edges but at higher concentrations tended to promote formation of multiple smaller spheroids. Similar morphologies were observed with the use of Matrigel (Figure 7F-H) with the protein content (Figure 7I) not showing evidence of altered growth over the culturing time. While the use of some additives positively influenced spheroid morphology, their ill-defined nature could produce more variability that would require additional characterisation.

Discussion and conclusion

Continuous cell lines, such as HepG2 cells, are considered more robust in maintaining their phenotype with maintenance of constant gene expression profile in low passage (Gómez-Lechón, Castell et al. 2007, Guo, Dial et al. 2010) which makes them advantageous in standardized preclinical models. Additionally, hepatocyte spheroids have been shown to be capable of mimicking higher order processes with functional hierarchical structures.

Spheroid formation of hepatoma cell lines (HepG2/C3A, PLC/PRF/5, and Hep3B) in hanging drops display three stages of assembly. Initial aggregation is followed by a delayed period for cadherin accumulation and compaction. Categorization based on differences in spheroid compactness define spheroid as compact, tight aggregates or loose cell associations. These categories closely link to expression of E-cadherin and N-cadherin (Lin, Chou et al. 2006, Ivascu and Kubbies 2007). Based on these correlations, the difference in morphology of HepG2 spheroids using cell stocks 1 to 3 from different sources, using the same technique, could be associated with variable expression and accumulation of essential cadherin's.

Maintenance and maturation of hepatocytes in spheroid cultures is advantageous but has shown high variability with respect to the complexity of the culture format. Size controlled spheroids produced by static hanging drops are amenable to high-throughput but the homogeneity of these spheroids when derived from an immortalized cell lines is ill-defined (Khetani and Bhatia 2008, Cai, DeLaForest et al. 2012, Wrzesinski, Rogowska-Wrzesinska et al. 2014). Producing spheroids for high-throughput hepatotoxicity assays, from any cellular origin, requires homogeneity and biological applicability. Hanging drops are advantageous as collection of multiple spheroids free of complex extracellular matrices can occur without hindrance. However, altering the seeding density, medium volume and extracellular matrix produced spheroids with wide-ranging end-point characteristics. In addition, the disparity across cell stocks and batches of immortalized cells contributes to divergent cellular responses and highlights concerns with generating reproducible characteristics in hanging drop spheroids. This research highlights features which result in varied characteristics of immortalised cells. This suggests a requirement for detailed analysing factors defining proliferative to stationary cell growth transitions of spheroids. Hanging drop cultures need to be compared to other spheroid models to establish whether more stable characteristics can be achieved or if the biological variance is similar across different three-dimensional cell culture platforms.

Conflict of interest

None of the authors declare any competing interests.

Author's contribution

TH and ADC designed and planned the experiments. TH, AE and ZFM performed the cell culture, downstream experimentation and statistical analysis. All authors contributed to the technical and biological interpretation of data and preparation of the manuscript.

Financial support

This work is based on the research supported in part by a National Research Foundation of South Africa Thuthuka grant (Grant No. 87880). Any opinion, finding, conclusion or recommendation expressed in this material is that of the author(s) and the NRF does not accept any liability in this regard.

References

Bhadriraju, K. and C. S. Chen (2002). "Engineering cellular microenvironments to improve cell-based drug testing." Drug Discovery Today **7**(11): 612-620.

Cai, J., et al. (2012). "Protocol for directed differentiation of human pluripotent stem cells toward a hepatocyte fate." StemBook.

Costa, A., et al. (2014). "An evaluation of the latest *in vitro* tools for drug metabolism studies." Expert Opinion on Drug Metabolism and Toxicology **10**(1): 103-119.

Fey, S. J. and K. Wrzesinski (2012). "Determination of drug toxicity using 3D spheroids constructed from an immortal human hepatocyte cell line." Toxicological Sciences **127**(2): 403-411.

Gómez-Lechón, M. J., et al. (2007). "Hepatocytes - the choice to investigate drug metabolism and toxicity in man: *In vitro* variability as a reflection of *in vivo*." Chemico-Biological Interactions **168**(1): 30-50.

Guo, L., et al. (2010). "Similarities and differences in the expression of drug metabolizing enzymes between human hepatic cell lines and primary human hepatocytes." Drug Metabolism and Disposition **39**(3): 528-538.

Härmä, V., et al. (2010). "A comprehensive panel of three-dimensional models for studies of prostate cancer growth, invasion and drug responses." PloS One **5**(5): 1-17.

Hirschhaeuser, F., et al. (2010). "Multicellular tumor spheroids: An underestimated tool is catching up again." Journal of Biotechnology **148**(1): 3-15.

Ivascu, A. and M. Kubbies (2006). "Rapid generation of single-tumor spheroids for high-throughput cell function and toxicity analysis." Journal of Biomolecular Screening **11**(8): 922-932.

Ivascu, A. and M. Kubbies (2007). "Diversity of cell-mediated adhesions in breast cancer spheroids." International Journal of Oncology **31**(6): 1403-1413.

Kelly, J. H. and G. J. Darlington (1989). "Modulation of the liver specific phenotype in the human hepatoblastoma line HepG2." In Vitro Cellular and Developmental Biology **25**(2): 217-222.

Kenny, P. A., et al. (2007). "The morphologies of breast cancer cell lines in three-dimensional assays correlate with their profiles of gene expression." Molecular Oncology **1**(1): 84-96.

Khetani, S. R. and S. N. Bhatia (2008). "Microscale culture of human liver cells for drug development." Nature Biotechnology **26**(1): 120-126.

Kim, J. B. (2005). "Three-dimensional tissue culture models in cancer biology." Seminars in Cancer Biology **15**(5): 365-377.

Kola, I. and J. Landis (2004). "Can the pharmaceutical industry reduce attrition rates?" Nature Reviews Drug Discovery **3**(8): 711-716.

Lin, R.-Z., et al. (2006). "Dynamic analysis of hepatoma spheroid formation: roles of E-cadherin and β1-integrin." Cell and Tissue Research **324**(3): 411-422.

Mehta, G., et al. (2012). "Opportunities and challenges for use of tumor spheroids as models to test drug delivery and efficacy." Journal of Controlled Release **164**(2): 192-204.

Nilesh, M., et al. (2011). Drug-Induced Hepatotoxicity, 2012.

Pampaloni, F., et al. (2007). "The third dimension bridges the gap between cell culture and live tissue." Nature Reviews Molecular Cell Biology **8**(10): 839-845.

Peters, T. S. (2005). "Do preclinical testing strategies help predict human hepatotoxic potentials?" Toxicologic Pathology **33**(1): 146-154.

Ryan, J., et al. (1975). "The influence of culture medium volume on cell density and lifespan of human diploid fibroblasts." Experimental Cell Research **91**(2): 389-392.

Selden, C., et al. (1999). "What keeps hepatocytes on the straight and narrow? Maintaining differentiated function in the liver." Gut **44**(4): 443-446.

Shin, J. W., et al. (2012). "Potential of engineering methodologies for the application to pharmaceutical research." Archives of Pharmacal Research **35**(2): 299-309.

Teng, Y. (2015). "Hanging Drop Aggregation Assay of Breast Cancer Cells." Cancer **5**(3).

Wrzesinski, K., et al. (2014). "The cultural divide: Exponential growth in classical 2D and metabolic equilibrium in 3D environments." PloS One **9**(9): 1-15.

Tables and Figures

Table 1:

Table 1: Mean values (±SEM) for cell cycle phases derived for spheroids (n =4) at variable seeding densities cultured for 7 days with the corresponding proliferation index.

	Sub-G1	**G1**	**S**	**G2/M**	**Proliferation index**
Monolayer control	5.37 ± 0.76	56.13 ± 0.84	24.55 ± 2.72	19.32 ± 1.96	43.87
Spheroids: 10000 cells	1.70 ± 0.89	73.60 ± 2.79	9.88 ± 4.27	16.52 ± 2.72	26.40
Spheroids: 20000 cells	0.87 ±0.26	68.41 ± 2.54	16.88 ± 4.79	14.71 ± 1.67	31.52
Spheroids: 40000 cells	1.65 ± 0.32	65.97 ± 4.33	19.10 ± 4.30	14.94 ± 1.47	34.03

Figure 1:

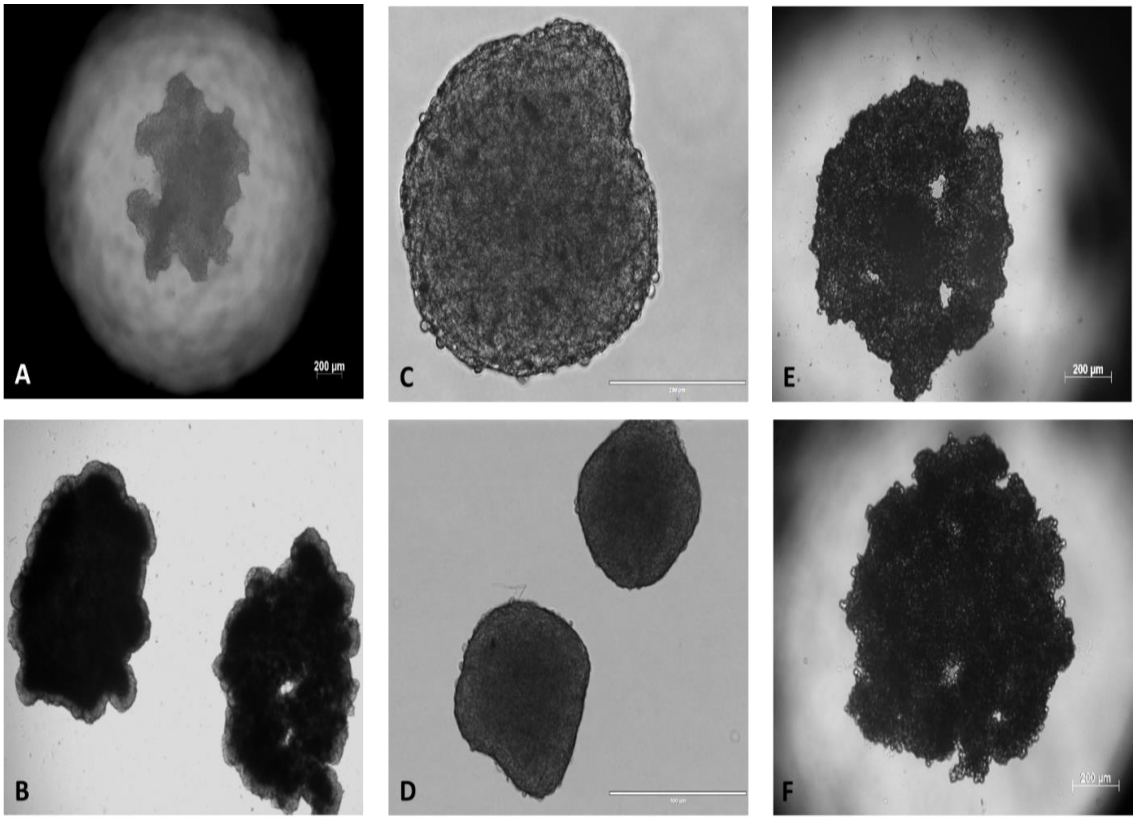

Figure 1: ***Spheroid morphology of different cell stocks.*** *Phase contrast images (EVOS FL Cell Imaging System* or Zeiss AX10 microscope*) of HepG2 spheroids seeded at 10 000 cells per well and culture for 10 days from A - B) Cell stock 1 with scale bar of 200 µm, C) Cell stock 2 with scale bar of 200 µm, D) Cell stock 2 with scale bar of 400 µm and E - F) Cell stock 3 with scale bar of 200 um.*

Figure 2:

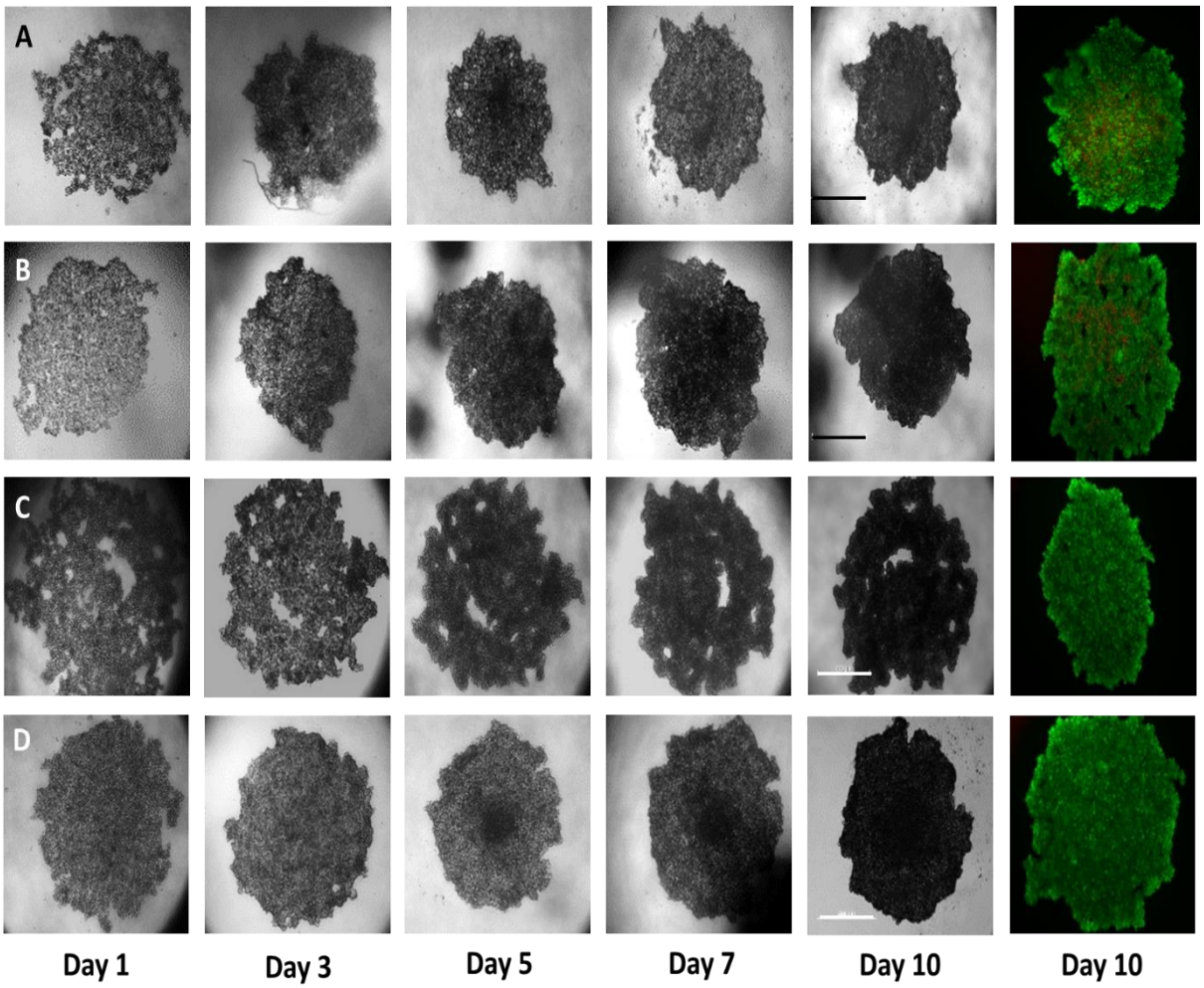

Figure 2: ***HepG2 spheroid morphology of the same spheroid over a 10 day time course.*** *Phase contrast images (Zeiss AX10 microscope) at seeding densities of A) Ten thousand cells per spheroid in 40 µl, B) Ten thousand cells per spheroid in 45 µl, C) Twenty thousand cells per spheroid in 40 µl and D) Twenty thousand cells per spheroid in 45 µl. Accompanying image of spheroids at Day 10 using Live-Dead staining with FDA-PI (Zeiss AX10 microscope). Scale bar: 500 µm.*

(Coloured, 2-column fitting image)

Figure 3:

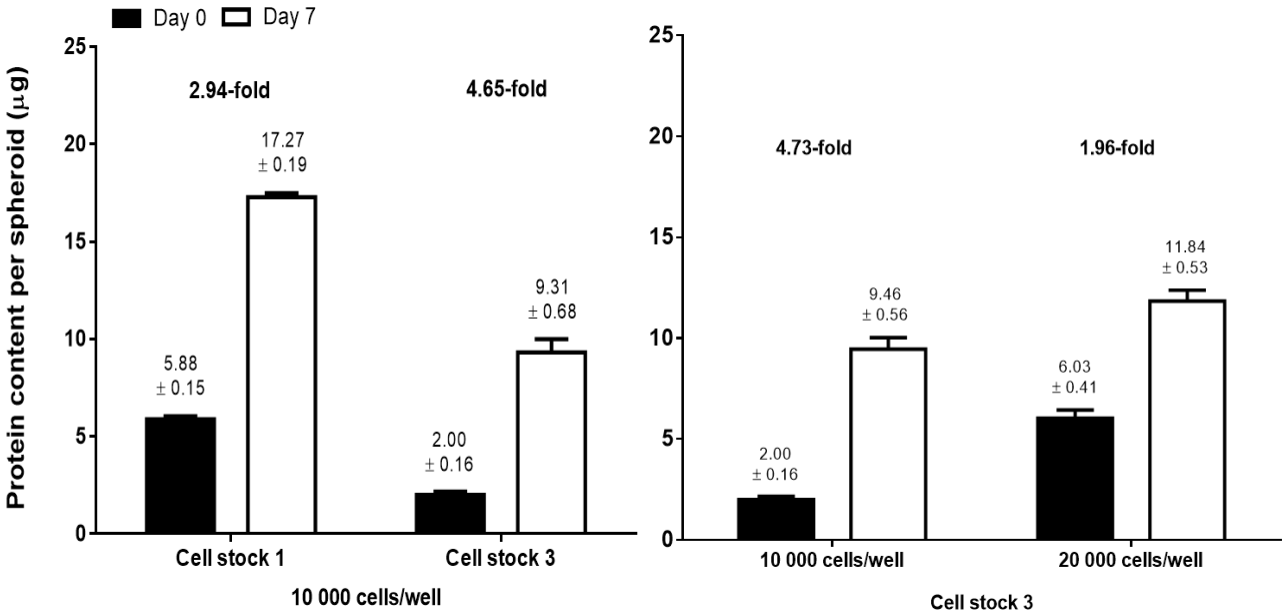

Figure 3: ***Relative protein content (micrograms) per spheroid from Day 0 to Day 7.*** *A) Cell stock 1 and cell stock 3, obtained from various source, were seeded at 10 000 cells per well in* forty-five microliters of *medium per drop and B) Cells from cell stock 3 seeded at densities of ten thousand and twenty thousand cells per well (technical duplicates, biological triplicates).*

(Coloured, 2-column fitting image)

Figure 4:

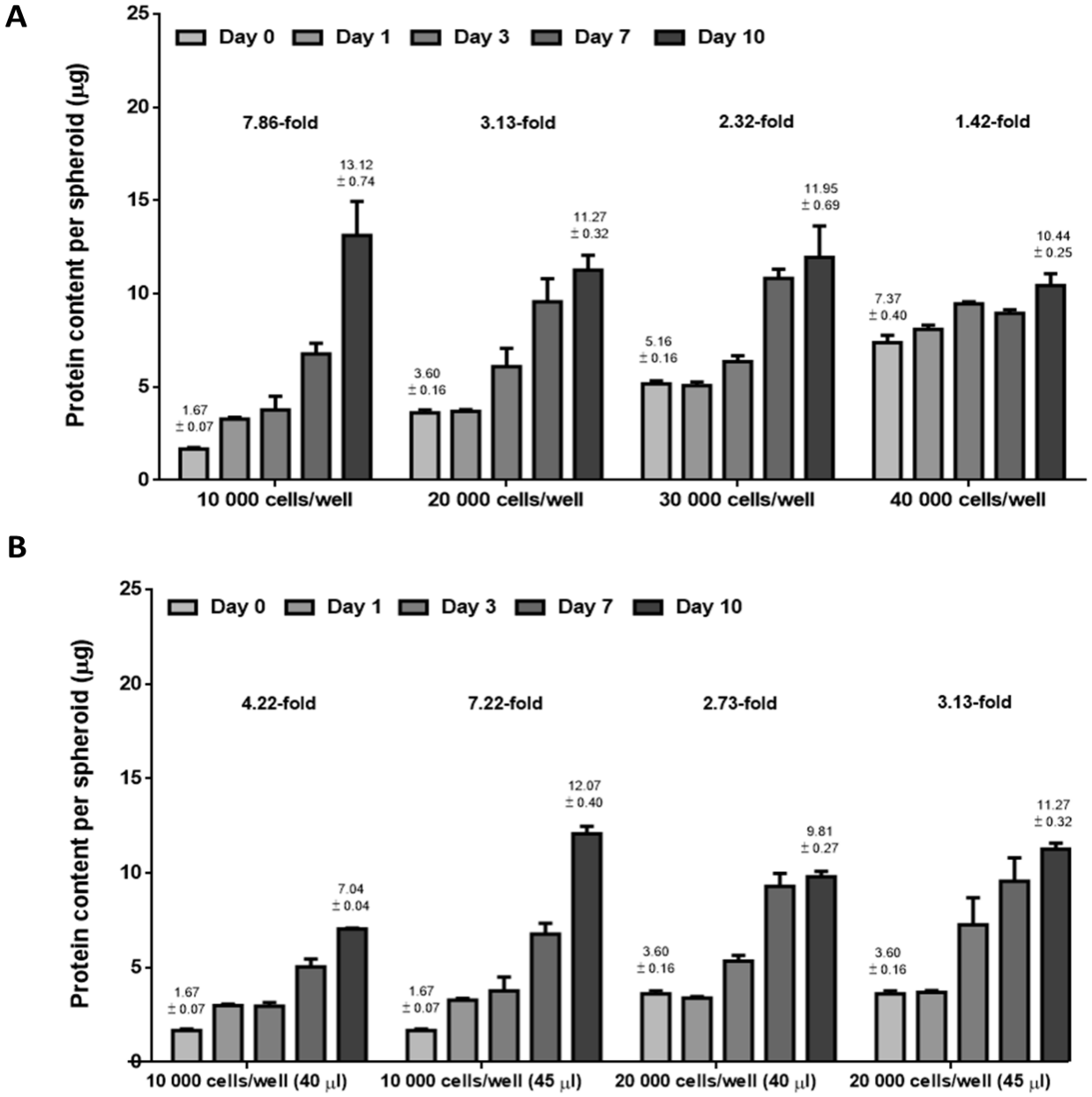

Figure 4: ***Relative protein content (micrograms) per spheroid over a time course of 10 days.*** *A) Variable seeding densities between ten thousand to forty thousand cells per well and B) Seeding densities of ten and twenty thousand cells per cell at variable volumes of forty and forty-five microliters of medium per drop (technical duplicates, biological triplicates).*

Figure 5:

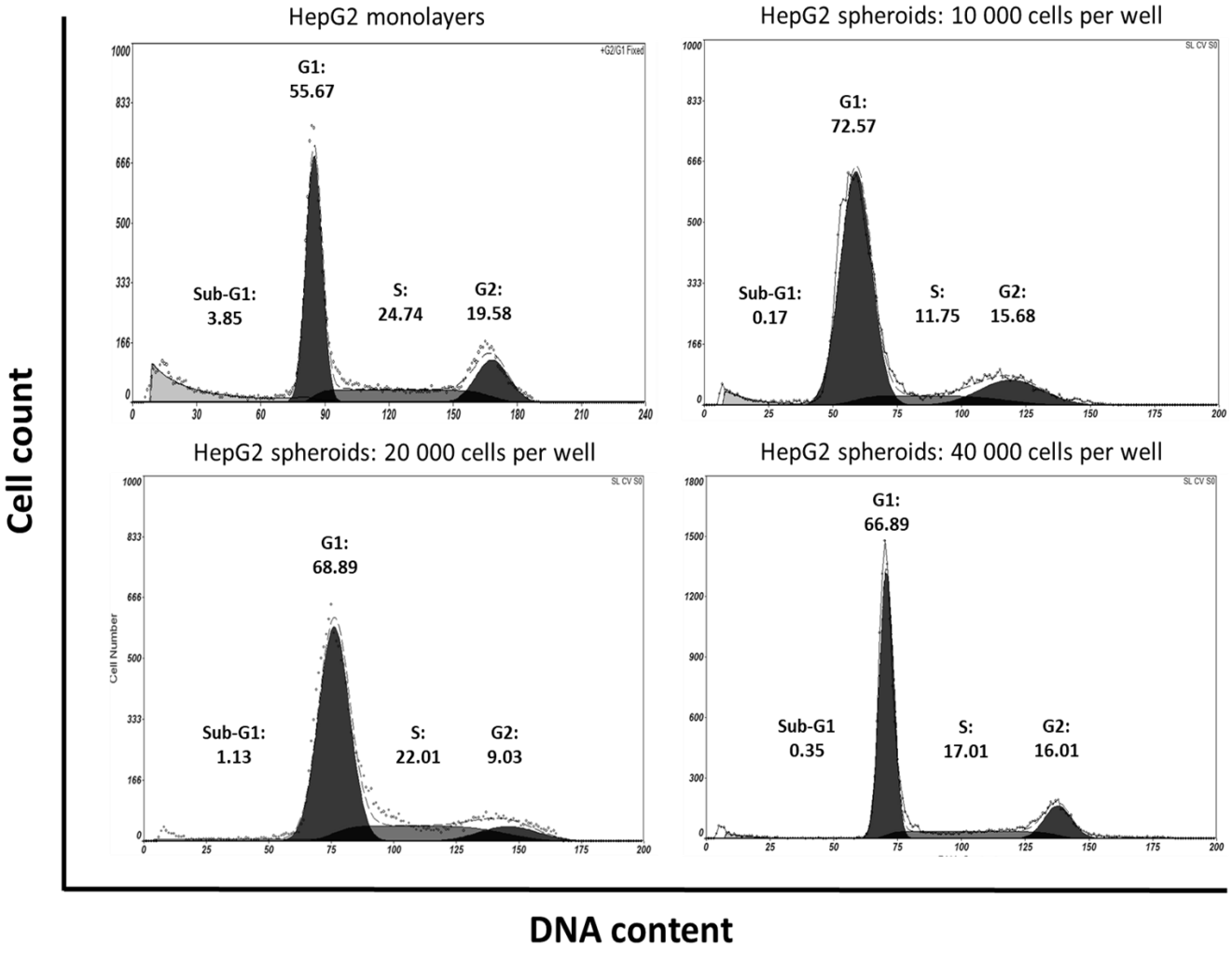

Figure 5: ***Cell cycle analysis of HepG2 monolayers and spheroids.*** *Deconvolution divided histograms into sub-G1 (cell debris and DNA fragments), G1 phase, S phase and G2/M phases with the percentage of each phase following deconvolution indicated. Spheroids seeded at 10 000, 20 000 and 40 000 cells per well in 45 µl and highlighted a stable sub-G1 population with no increase in cell death in HepG2 spheroids and an increase in the G1 population of HepG2 spheroids associated with cell quiescence and increased doubling time. The mean of each phase of the cell cycle for n = 4 experiments correlating to these histograms is included in Table 1.*

(Coloured, 2-column fitting image)

Figure 6:

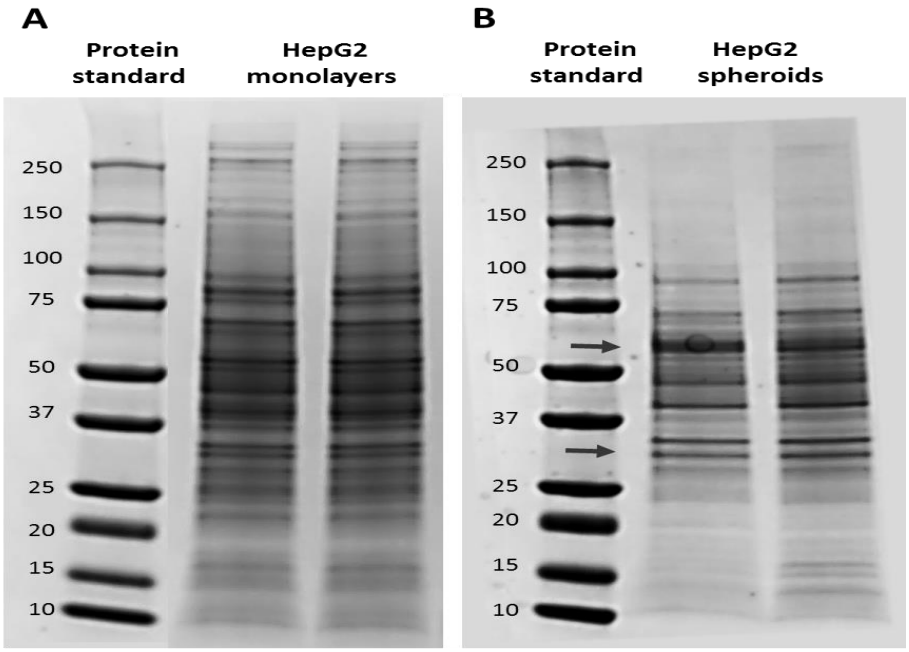

Figure 6: ***Protein mass profiles of Hepg2 monolayers and spheroids.*** *Coomassie stained 4-15% Mini-PROTEAN TGX gel of A) HepG2 monolayers and B) HepG2 spheroids with differences in protein-mass profiles being evident between 25 - 37 kDa and 50 - 75 kDa.*

(Black and white, 2-column fitting image)

Figure 7:

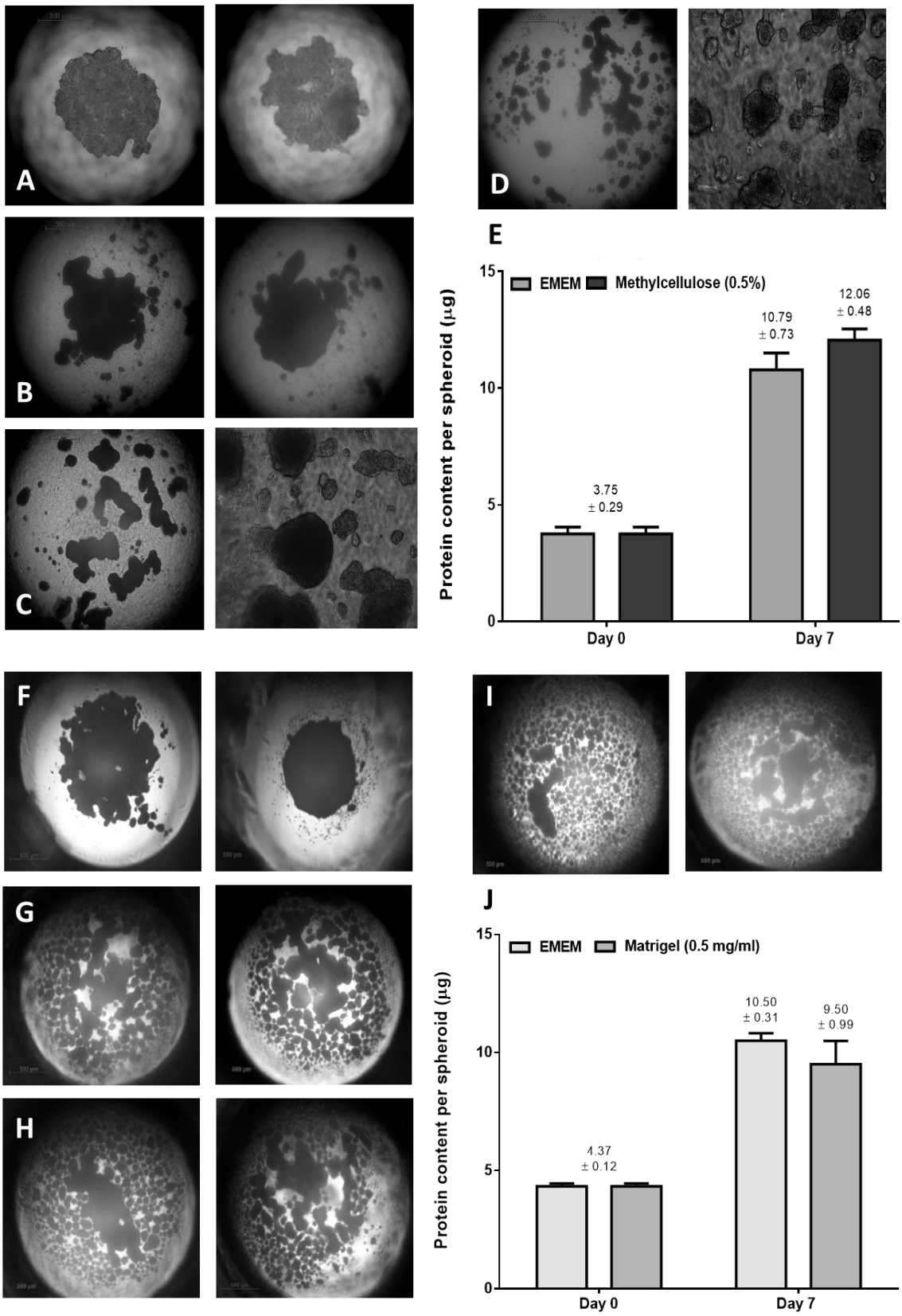

Figure 7: ***Influence of extracellular matrix on spheroids.*** *Phase contrast images (Zeiss inverted Axiovert CFL40 microscope, scale bar: 500 µm) of HepG2 cell (10 000 or 20 000 cells per well) cultured in hanging drops with variable medium additives: A) Medium only, B) 0.5% methylcellulose, C) 1% methylcellulose, D) 2% methylcellulose, E) Relative protein content (micrograms) per spheroid over 7 days, F) 0.5 mg/ml Matrigel, G) 1.0 mg/ml Matrigel, H) 2.0 mg/ml and I) 4.0 mg/ml Matrigel and J) Relative protein content (micrograms) per spheroid over 7 days (technical duplicates, biological triplicates).*

(Coloured, 2-column fitting image)

Supplementary data

Supplementary Figure 1

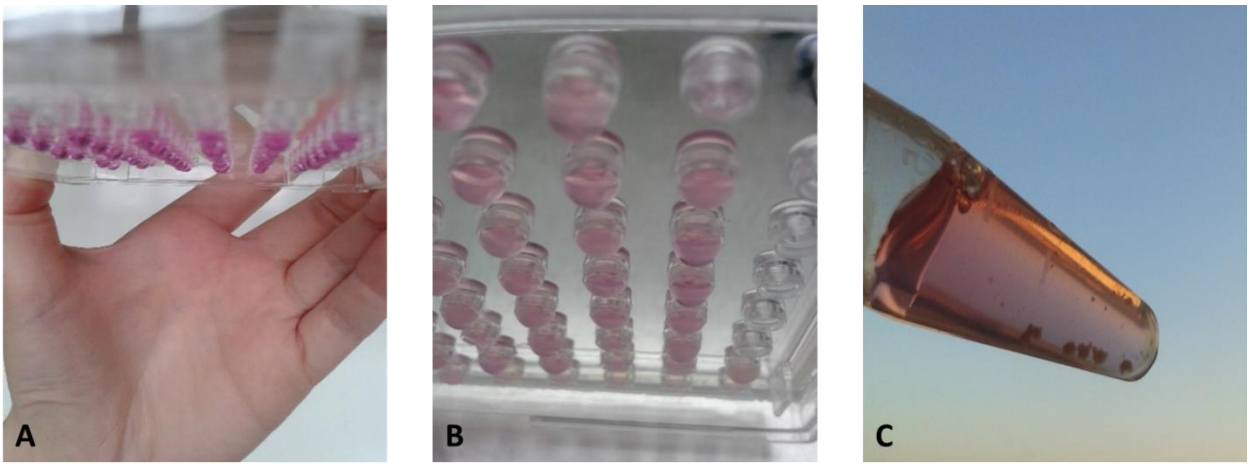

Figure 1: ***Photographs of HepG2 cells****. A and B) Seeded in hanging-drop plates C) Harvested into an Eppendorf tube at Day 15.*
(Coloured, 2-column fitting image)

Supplementary Figure 2

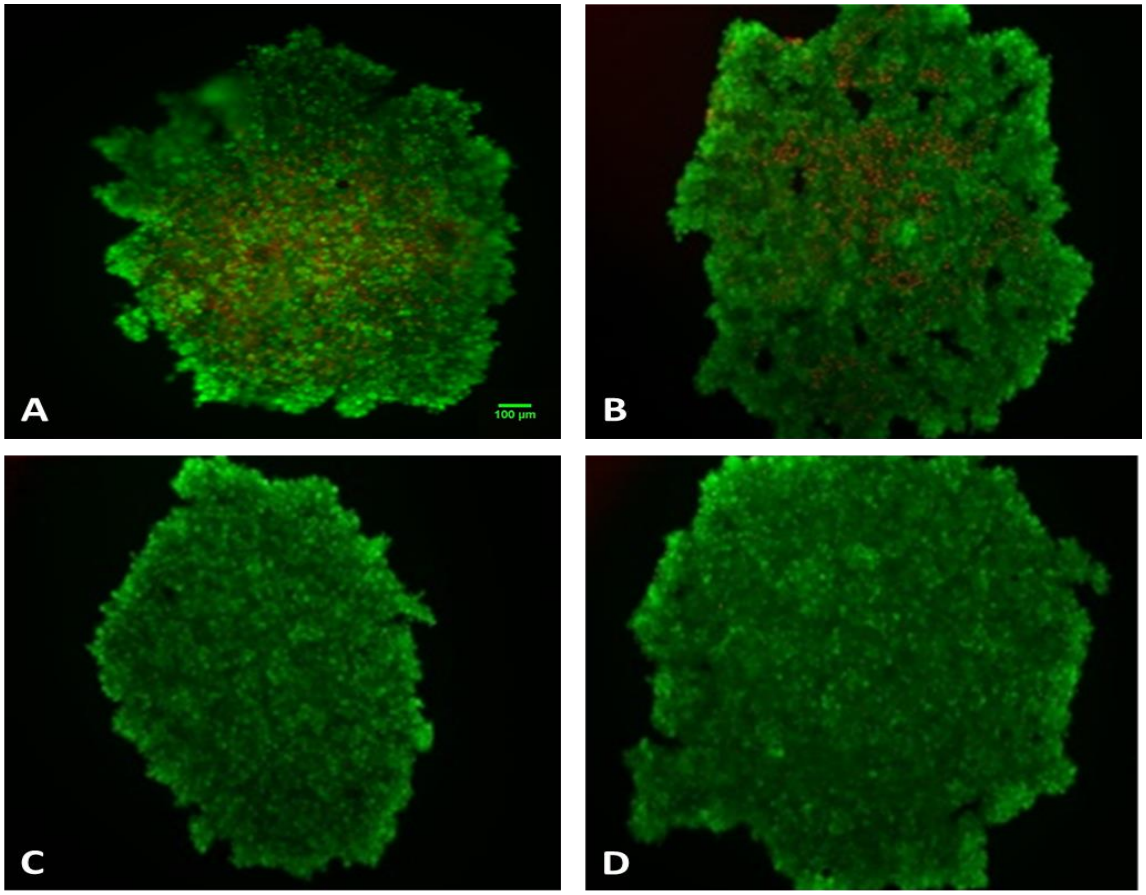

Figure 2: ***HepG2 spheroid viability illustrated by fluorescent microscopy*** *(Zeiss AX10 microscope). A) Ten thousand cells per spheroid in 40 µl, B) Ten thousand cells per spheroid in 45 µl, C) Twenty thousand cells per spheroid in 40 µl and D) Twenty thousand cells per spheroid in 45 µl.*
(Coloured, 2-column fitting image)